

Report

LA-ICP-MS U–Pb dating of the 401 apatite

Shogo AOKI[1, 2*], Yuki DATE[3], Hirotsugu NISHIDO[4] & Kazumasa AOKI[1]

Abstract: We performed apatite uranium–lead (U–Pb) analysis on an age standard sample (401 apatite; ca. 530 Ma) using laser ablation inductively coupled plasma mass spectrometer (LA-ICP-MS). As a result, intercept ages on Tera–Wasserburg concordia (TW) diagram by drawing a regression line from the data yielded 553.6 ± 6.7 Ma, which was significantly older than the reference age. On the other hand, the regression line from the data anchored through an initial common Pb isotopic ratio yielded a lower intercept age of 538.0 ± 8.2 Ma. In addition, the weighted-mean ^{207}Pb-correction age calculated from each data was 537.1 ± 8.1 Ma. These are consistent with the reference age. Accordingly, it was confirmed that the correction methods assuming initial common Pb isotopic composition were effective for calculating accurate apatite U–Pb ages in the case of small U/Pb and Pb isotopic ratio variations.

I. Introduction

Apatite [$Ca_{10}(PO_4)_6(OH, F, Cl)_2$] is a uranium (U)-bearing accessory mineral in igneous and metamorphic rocks, and a minor but widespread detrital component in clastic sedimentary rocks. The bones and teeth of fossil animals also contain apatite. The uranium–lead (U–Pb) apatite system has a closure temperature of approximately 450°C-550°C (Chamberlain & Bowring 2001, Schoene & Bowring 2007) and tends to be resistant to post-geological alteration (Chamberlain & Bowring 2001). Thus, *in-situ* apatite U–Pb geochronology using laser ablation inductively coupled plasma mass spectrometry (LA-ICP-MS) or secondary-ion mass spectrometry (SIMS) is a reliable method for providing timescale information associated with sedimentary, igneous, metamorphic and fossilized processes (e.g. Sano & Terada 1999, Sano et al. 2006, Tütken et al. 2008, Chew et al. 2011, Kirkland et al. 2018). However, precise apatite U–Pb age is commonly hindered by low U or Pb concentrations and high common Pb/radiogenic Pb ratios that require common Pb correction. This correction typically requires two steps: (1) data plots on a suite of co-genetic apatite grains or domains with a large spread in common Pb/radiogenic Pb ratio and (2) adopting the appropriate initial common Pb isotopic composition. One such correction method involves a projecting an intercept through the uncorrected data on a Tera–Wasserburg (TW) concordia diagram to determine the common Pb-component (y-intercept) on the ^{207}Pb/^{206}Pb axis. Thereafter, the U–Pb age is calculated either as a lower intercept age on a concordia curve, or as a weighted mean ^{207}Pb-corrected ages using the ^{207}Pb/^{206}Pb intercept as an estimate of the initial Pb isotopic composition. Another approach is plotting the uncorrected data on a TW diagram but anchoring the intercept through the initial Pb isotopic composition using either the Stacey & Kramers (1975)'s model for crustal Pb evolution or independent constraints by analyzing a low-U and co-magmatic phase, e.g. K-feldspar and plagioclase. Hence, the apatite U–Pb analysis is extremely sensitive, and requires both high reliability and productivity in a short time. The Okayama University of Science (OUS) introduced LA-ICP-MS as part of the Private University Research Branding Project in 2018. In the current study, to verify whether a precise *in-situ* apatite U–Pb age can be obtained using LA-ICP-MS in OUS, we performed analyses on the 401 apatite standard (530.3 ± 1.5 Ma; Thompson et al. 2016).

II. Standard Samples

We prepared two apatite standards of OD306 and 401. The OD306 apatite was used as an external standard for the correction of the U/Pb ratios of the 401 apatite in this study. The OD306 was collected from an apatite-magnetite vein at the Acropolis copper-gold prospect in South

[1.] 岡山理科大学基盤教育センター,〒700-0005 岡山県岡山市北区理大町1-1. Center for Fundamental Education, Okayama University of Science, 1-1 Ridai-cho, Kita-ku, Okayama 700-0005, Japan.
[2.] 秋田大学国際資源学部,〒010-8502 秋田県秋田市手形学園町1-1. Faculty of International Resource Sciences, Akita University, 1-1 Tegatagakuen-machi, Akita 010-8502, Japan.
[3.] 岡山理科大学理学部基礎理学科,〒700-0005 岡山県岡山市北区理大町1-1. Department of Applied Science, Okayama University of Science, 1-1 Ridai-cho, Kita-ku, Okayama, 700-0005, Japan.
[4.] 岡山理科大学生物地球学部生物地球学科,〒700-0005 岡山県岡山市北区理大町1-1. Faculty of Biosphere-Geosphere Science, Okayama University of Science, 1-1 Ridai-cho, Kita-ku, Okayama, 700-0005, Japan.
*Correspondence: Shogo AOKI, E-mail: s.aoki.nulliak@gmail.com

Australia (Huang et al. 2015). The U–Pb dating by ID-MC-ICP-MS yielded a lower intercept at 1596.7 ± 7.1 Ma (2σ uncertainties) on a TW plot (Thompson et al. 2016). The 401 apatite used in this study was a megacryst collected in Iran (Thompson et al. 2016). The U–Pb age of the apatite 401 by ID-MC-ICP-MS defined a regression with a lower-intercept age of 530.3 ± 1.5 Ma (2σ) on a TW diagram (Thompson et al. 2016). Also, NIST SRM612 glass (Jochum et al. 2005) was analyzed as the external standard for the correction of the $^{207}Pb/^{206}Pb$ ratios of the 401 apatite. All standards were mounted and polished on 6-mm acrylic disks prior to their analysis.

III. Analytical Method

In-situ U–Pb measurement was conducted in OUS using a Thermo Fisher Scientific iCAP-RQ single-collector quadrupole ICP-MS combined with a Teledyne Cetac Technologies Analyte G2 laser ablation (LA) system that utilizes a 193-nm argon fluoride (ArF) excimer laser. The standard materials were set in a two-volume HelEx2 sample cell of the LA system. The ICP-MS was optimized using continuous ablation of a NIST SRM 612 glass to provide the maximum sensitivities of ^{206}Pb and ^{238}U while maintaining low oxide formation ($^{232}Th^{16}O/^{232}Th < 1\%$). At the start of each session, the laser fluence was set to 1.72 J/cm^2 at the sample surfaces with a laser repetition rate and laser diameter set to 5 Hz and 35 μm, respectively. After laser shooting with shutter closed for 30 s (laser warming up), the analytical areas were ablated for 30 s. Helium (He) gas was introduced into the HelEx2 sample cell (MFC1) and into its arm part (MFC2) as a carrier gas. The flow rate into the MFC1 and the MFC2 was set to 0.5 L/min and 0.3 L/min, respectively. The ablated materials of the samples in the He carrier gas were mixed with Ar gas (at a flow rate of 0.9 L/min) and passed through a baffled-type signal-smoothing device (Tunheng & Hirata 2004) into the ICP-MS. Prior to conducting the analysis, to avoid analytical uncertainty, we chose analytical regions without cracks and inclusions by referring to CL images and observations with the LA camera in reflected and transmitted light. In addition, the analyzed spots were ablated using a pulse of the laser with a diameter of 50 μm to remove potential contaminants on their surfaces.

The analyzed masses included six nuclides of ^{202}Hg, ^{204}Pb, ^{206}Pb, ^{207}Pb, ^{232}Th and ^{238}U. The background and ablation data for each analysis were collected for 15 s of the laser warming-up time and 20 s of the ablation time, respectively. The background intensities were subtracted from the subsequent intensities at the ablation. These data were acquired for multiple analyses of the 401 apatite, bracketed by each three analysis of the OD306 apatite and NIST SRM 612 glass. As normalization values for the OD306 apatite, the radiogenic $^{206}Pb/^{238}U$ ratio was calculated by correction based on the assumption that its common Pb isotopic ratio was equal to the terrestrial Pb isotopic ratio of 1596.7 Ma (based on the model by Stacey & Kramers 1975). The $^{207}Pb/^{206}Pb$ ratio was corrected by normalizing to the compiled values of NIST SRM 612 glass standard by Jochum et al. (2005). All uncertainties concerning Pb/U elemental and Pb isotopic ratios were quoted at a 2-sigma level, to which the repeatability of external standard data of the OD306 apatite and the NIST SRM 612 glass bracketing analyses of the 401 apatite was propagated based on quadratic addition. The ^{235}U intensities were calculated from ^{238}U using a $^{238}U/^{235}U$ ratio of 137.818 (Hiess et al. 2012). Data were reduced using Thermo Scientific Qtegra Intelligent Scientific Data Solution (ISDS) platform software, with normalization and uncertainty propagation calculated offline using an in-house Microsoft Excel spreadsheet. A summary of analytical conditions is given in Table 1.

The age of the 401 apatite was calculated using Isoplot/Ex 4.15 (Ludwig 2012, and its update) based on the following independent three methods; (1) calculating the lower intercept on the TW concordia curve by drawing a regression line based on the data, (2) determining a lower intercept age from the intersection of the TW concordia curve and a regression line from the data, anchored through common Pb, and (3) calculating weighted-mean ^{207}Pb-correction age. Although the ^{204}Pb- and ^{208}Pb-correction methods were also employed for common Pb correction (e.g. Cocherie et al. 2009), these methods have been less commonly applied compared with those using ^{207}Pb-correction one. Hence, we only used the ^{207}Pb-correction method in this study. In terms of the methods (2) and (3), the initial common Pb isotopic ratio was assumed to be the terrestrial isotopic ratio of 530.3 Ma provided by Stacey & Kramers (1975)'s model.

IV. Result and Discussion

Sixteen spots were analyzed in the 401 apatite, and the results are listed in Table 2. Figure 1 shows a TW concordia plot of each of the data made with Isoplot/Ex 4.15 (Ludwig 2012, and its update). The unanchored TW intercept age (method 1) yielded 553.6 ± 6.7 Ma (MSWD = 0.73; Fig. 1A), which is significantly older than the reference age of 530.3 ± 1.5 Ma. On the other hand, the anchored TW intercept age (method 2) and the ^{207}Pb-corrected age (method 3) yielded

Table 1. Summary of analytical procedure and data reduction scheme for apatite U–Pb dating by LA-ICP-MS.

Laser ablation system	
Instrument	ArF Excimer Laser Analyte G2 (Teledyne Cetac Technologies, Omaha, USA)
Cell type	HelEx 2-volume sample chamber
Laser wave length	193 nm
Pulse duration	<5 ns
Fluence	1.72 J/cm^2
Repetition rate	5 Hz
Laser diameter size	35 μm (circular spot)
Sampling mode	Single hole drilling
Pre-cleaning	1 shot with diameter size of 50 μm
Carrier gas	He gas and Ar make-up gas combined outside ablation cell
He gas flow rate	
Flow rate into sample cell "MFC1"	0.5 l/min
Flow rate into the HelEx arm "MFC2"	0.3 l/min
Ar make-up gas flow rate	0.986 l/min
Laser warming-up (laser shooting with laser shutter closed) duration	30 s
Ablation duration	30 s
Signal smoothing device	baffled-type device (Tunheng & Hirata 2004)
ICP Mass Spectrometer	
Instrument	iCAP-RQ (Thermo Fisher Scientific, USA)
RF power	1550 W
Data reduction	Integration of total ion counts per single ablation. Signals obtaind from first few seconds were not used for data reduction, and next signals obtained from 20 s were integrated for further calculations. Signal intensity of ^{235}U was not monitored and ^{207}Pb/^{235}U is calculated assuming ^{238}U/^{235}U = 137.818 (Hiess et al. 2012).
Detection mode	Pulse counting mode by a secondary electron multiplier
Monitored mass peak	^{202}Hg, ^{204}(Hg + Pb), ^{206}Pb, ^{207}Pb, ^{232}Th, ^{238}U
Integration time per mass peak	0.01 s for ^{202}Hg and ^{204}(Hg + Pb), 0.5 s for ^{206}Pb and ^{207}Pb, 0.01 s for ^{208}Pb, 0.01 s for ^{232}Th and 0.5 s for ^{238}U
Data processing	
Background correction	Background counts were obtained for 15 s of laser warming-up time, and ablation signals were subtracted from the background counts
Calibration strategy	The OD306 was used for correction of Pb/U in all measurements. The NIST SRM 612 was used for correction of Pb/Pb and U/Pb fractionation. All correction factor for elemental and isotopic fractionation are determined by linear interpolation.
Normalization values	Calculated radiogenic Pb/U ratios of the OD306 were used based on common Pb isotopic ratios using model by Stacey & Kramers (1975). Pb isotopic ratios of The NIST SRM 612 by Jochum et al. (2005) were used.
Uncertainties	Uncertainties and isotope ratios were quoted at 2 SD absolute to which repeatability of each six analyses of the OD306 apatite and the NIST SRM 612 bracketing multiple analyses of the 401 apatite were propagated.

Table 2. Summary of the U–Pb isotopic and ^{207}Pb-corrected age data of the 401 apatite.

Spot No.	^{207}Pb/^{235}U	2σ	^{206}Pb/^{238}U	2σ	^{207}Pb/^{206}Pb	2σ	^{207}Pb-corrected age	
							Age (Ma)	2σ
1	0.8609	0.0732	0.0872	0.0020	0.0716	0.0059	530.6	12.43
2	0.7927	0.0703	0.0864	0.0020	0.0666	0.0057	528.8	12.28
3	0.7088	0.0681	0.0900	0.0020	0.0571	0.0053	556.6	12.75
4	0.8962	0.0711	0.0841	0.0022	0.0773	0.0058	508.3	13.73
5	0.7693	0.0706	0.0870	0.0023	0.0642	0.0056	534.0	14.31
6	0.7904	0.0687	0.0864	0.0023	0.0664	0.0055	528.6	14.16
7	0.7806	0.0806	0.0883	0.0032	0.0641	0.0062	542.0	19.78
8	0.8400	0.0839	0.0891	0.0033	0.0684	0.0064	543.5	19.90
9	0.7760	0.0818	0.0894	0.0033	0.0630	0.0062	548.8	20.06
10	0.8596	0.0852	0.0861	0.0032	0.0724	0.0067	523.4	19.34
11	0.8645	0.0853	0.0863	0.0032	0.0727	0.0067	524.1	19.29
12	0.7970	0.0788	0.0919	0.0033	0.0629	0.0058	564.1	20.08
13	0.7584	0.0759	0.0876	0.0027	0.0628	0.0060	538.2	16.88
14	0.6863	0.0729	0.0896	0.0021	0.0555	0.0058	555.5	13.18
15	0.7318	0.0756	0.0897	0.0031	0.0592	0.0058	553.4	19.03
16	0.7631	0.0777	0.0862	0.0032	0.0643	0.0061	528.9	19.28

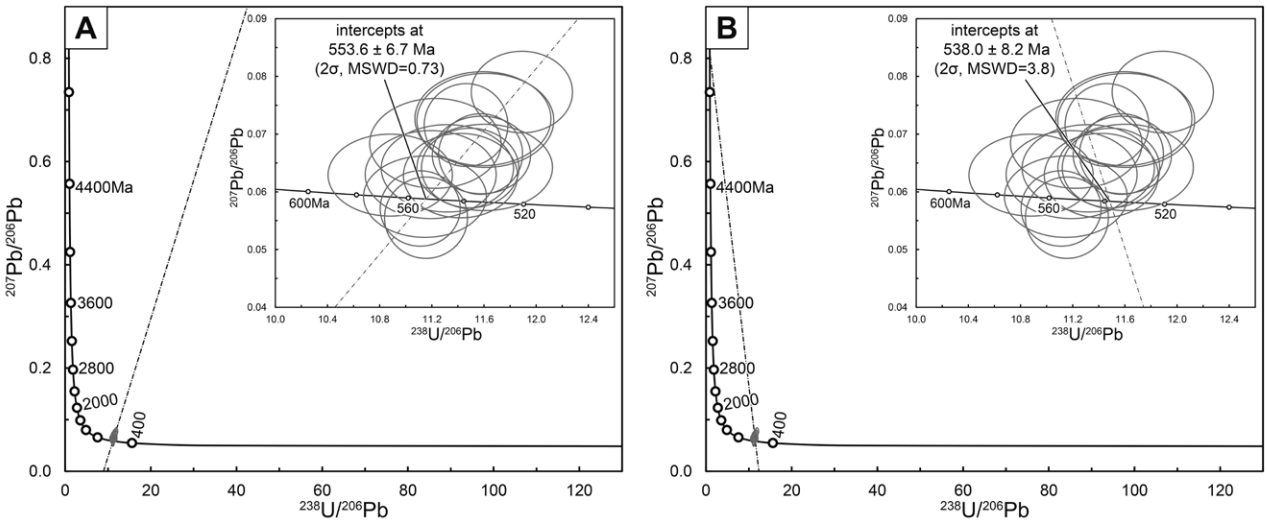

Fig. 1. Tera-Wasserburg concordia diagrams for the 401 apatite. (A) unanchored and (B) anchored initial common Pb isotopic composition.

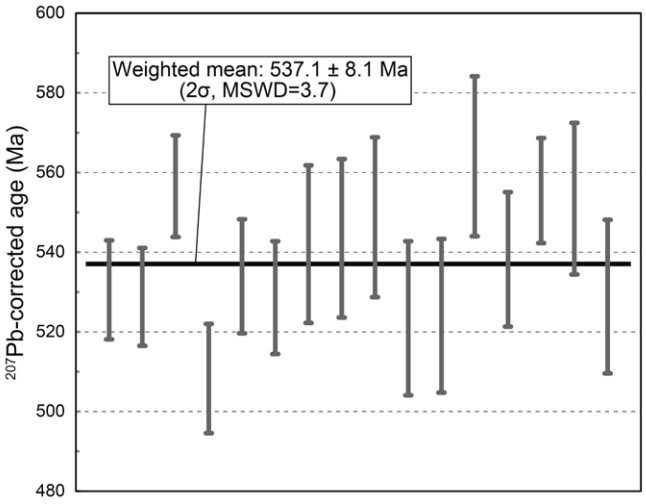

Fig. 2. Weighted mean ^{207}Pb-corrected age of the 401 apatite.

538.0 ± 8.2 Ma (MSWD = 3.8; Fig. 1B) and 537.1 ± 8.1 Ma (MSWD = 3.7; Fig. 2), respectively, which are consistent with the reference age reported by Thompson et al. (2016).

The inaccurate result showing the unanchored TW intercept age was caused by the data with a small spread in the common Pb/radiogenic Pb ratio in the TW plot because the regression line could not be properly defined in this situation. In fact, the slope of the regression line is typically negative, while, for our data, it is positive. Conversely, the ages obtained from using the remaining two methods were equal and consistent with the reference age of 530.3 ± 1.5 Ma, indicating that the U/Pb and Pb isotopic ratios could be measured precisely and accurately in our analytical condition. This was possible because the initial common Pb isotopic ratio was used as the terrestrial isotopic ratio of 530.3 Ma (Stacey & Kramers 1975) and the ^{207}Pb-corrected age was a projection through the common Pb onto the ^{238}U/^{206}Pb axis of the TW diagram (Chew et al. 2011). If the accuracy of our data was low, the above results would be not achieved. Thus, we can argue that precise apatite U–Pb dating can be conducted using an LA-ICP-MS system under the analytical condition described in section III and shown in Table 1.

Our study was able to verify that methods 2 and 3 using common Pb isotopic ratios had been effective for precise apatite U–Pb dating with small variations in U/Pb and Pb isotopic ratios. As previously noted, apatite is commonly observed in samples in a variety of fields such as geology, paleontology and archaeology. Those unknown apatite samples are empirically known to have small variations of U/Pb and Pb isotopic ratios, similar to the 401 apatite in this study. According to Chew et al (2011), ^{207}Pb-corrected age is not dependent on the choice of initial age applied to common Pb. Additionally, the authors proposed an iterative approach combined with the model

of Stacey & Kramers (1975). This approach was repeated five times and the difference between the ^{207}Pb-corrected age and the initial age became negligibly small. Accordingly, we aim to apply these methods combined with the repetition approach (Chew et al. 2011) for unknown apatite samples in a variety of fields using the LA-ICP-MS system in OUS.

Acknowledgements

We are grateful to S. Sakata for his critical advice, which improved LA-ICP-MS analytical conditions and developed the calculation program of mineral U–Pb age data. This study was financially supported by Private University Research Branding Project (OUS) and JSPS KAKENHI Grant Number JP19K04043 (K.A.).

References

Chamberlain, K. R. & Bowring, S. A. (2001) Apatite-feldspar U–Pb thermochronometer: a reliable, mid-range (~450°C), diffusion-controlled system. Chemical Geology 172: 173-200.

Cocherie, A., Fanning, C. M., Jezequel, P. & Roberta, M. (2009) LA-MC-ICPMS and SHRIMP U–Pb dating of complex zircons from Quaternary tephras from the French Massif Central: Magma residence time and geochemical implications. Geochimica et Cosmochimica Acta 73: 1095-1108.

Chew, D. M., Sylvester, P. J. & Tubrett, M. N. (2011) U–Pb and Th–Pb dating of apatite by LA-ICPMS. Chemical Geology 280: 200-216.

Hiess, J., Condon, D. J., McLean, N. & Noble, S. R. (2012) ^{238}U/^{235}U systematics in terrestrial uranium-bearing minerals. Science 335: 1610-1614.

Huang, Q., Kamenetsky, V. S., McPhie, J., Ehrig, K., Meffre, S., Maas, R., Thompson, J., Kemenetsky, M., Chambefort, I., Apukhtina, O. & Hu, Y. (2015) Neoproterozic (ca. 820-830 Ma) mafic dykes at Olympic Dam, South Australia: Links with the Gairdner Large Igneous Province. Precambrian Research 271: 160-172.

Jochum, K. P., Pfänder, J., Woodhead, J. D., Willbold M., Stoll, B., Herwig, K., Amini, M., Abouchami, W. & Hofmann, A. W. (2005) MPI-DING glasses: New geological reference materials for in situ Pb isotope analysis. Geochemistry Geophysics Geosystems 6: Q10008.

Kirkland, C. L., Yakymchuk, C., Szilas, K., Evans, N., Hollis, J., McDonald, B. & Gardiner, N. J. (2018) Apatite: a U-Pb thermochronometer or geochronometer?. Lithos 318-319: 143-157.

Ludwig, K. (2012) User's Manual for Isoplot 3.75: A geochronological toolkit for Microsoft Excel. Berkeley Geochronology Center Special Publication, no. 5, Berkley.

Sano, Y. & Terada, K. (1999) Direct ion microprobe U–Pb dating of fossil tooth of a Permian shark. Earth and Planetary Science Letters 174: 75-85.

Sano, Y., Terada, K., Ly, C. V. & Park, E. J. (2006) Ion microprobe U-Pb dating of a dinosaur tooth. Geochemical Journal 40: 171-179.

Schoene, B. & Bowring, S. A. (2007) Determining accurate temperature-time paths from U–Pb thermochronology: An example from the Kaapvaal craton, southern Africa. Geochimica et Cosmochimica Acta 71: 165-185.

Stacey, J. S. & Kramers, J. D. (1975) Approximation of terrestrial lead isotope evolution by a two-stage model. Earth and Planetary Science Letters 26: 207-221.

Thompson, J., Meffre, S., Maas, R., Kamenetsky, V., Kamenetsky M., Goemann, K., Ehrig, K. & Danyushevsky, L. (2016) Matrix effects in Pb/U measurements during LA-ICP-MS analysis of the mineral apatite. Journal of Analytical Atomic Spectrometry 31: 1206-1215.

Tunheng, A. & Hirata T. (2004) Development of signal smoothing device for precise elemental analysis using laser ablation-ICP-mass spectrometry. Journal of Analytical Atomic Spectrometry 19: 932-934.

Tütken, V., Vennemann, T. W. & Pfretzschner, H. U. (2008) Early diagenesis of bone and tooth apatite in fluvial and marine settings: Constraints from combined oxygen isotope, nitrogen and REE analysis. Palaeogeography, Pelaeoclimatology, Palaeoecology 266: 254-268.

青木翔吾・伊達勇輝・西戸裕嗣・青木一勝：LA-ICP-MSを使った401アパタイトのU–Pb年代測定

要約

本論では，岡山理科大学に導入されたレーザーアブレーション誘導結合プラズマ質量分析器を使い，年代既知のアパタイト（401アパタイト; 約530 Ma）のU–Pb年代測定を行なった．その結果，Terra-Wasserburg (TW) 図上に、初生鉛の値を固定せず測定データから回帰線を求めた場合，553.6 ± 6.7 Maという年代値を示した．一方，初生鉛値を固定し回帰線を求めた場合は，538.0 ±8.2 Maという年代値が得られ，推奨年代値と一致した．さらに，207鉛補正を行った１つ１つのデータから加重平均年代値を求めたところ，537.1 ± 8.1 Maという値が得られ，これも推奨年代値と一致した．これらのことから，TW図上においてU/Pb比とPb同位体比のばらつきが小さい試料については，初生鉛を補正する年代計算手法が有効であることが確認できた．

(Accepted 10 November 2020)